

Undamped transverse electric mode in undoped two-dimensional tilted Dirac cone materials

Z. Jalali-Mola^{1,*} and S. A. Jafari^{1,2,†}

¹Department of Physics, Sharif University of Technology, Tehran 11155-9161, Iran

²Center of Excellence for Complex Systems and Condensed Matter (CSCM), Sharif University of Technology, Tehran 1458889694, Iran



(Received 26 February 2020; accepted 26 October 2020; published 29 December 2020)

Transverse electric (TE) modes cannot propagate through the conducting solids. This is because the continuum of particle-hole excitations of conductors contaminates with the TE mode which damps it out. But in solids hosting tilted Dirac cone that admit a description in terms of a modified Minkowski space-time, the new space-time structure remedies this issue and therefore a tilted Dirac cone material (TDM) supports the propagation of an undamped TE mode which is sustained by charge density fluctuations. The resulting TE mode propagates at *fermionic velocities* v_F , which implies (i) it is strongly confined to the surface of the two-dimensional (2D) TDM and (ii) the TDM acts as a high refractive index $n = c/v_F \sim 10^2$ medium for TE modes.

DOI: [10.1103/PhysRevB.102.245148](https://doi.org/10.1103/PhysRevB.102.245148)

I. INTRODUCTION

Electromagnetic waves in the vacuum and dielectrics can propagate as both TE and transverse magnetic (TM) modes [1]. When they hit a conductor, the TM mode organizes itself into collective motions of the density known as plasmons [2–5]. But the TE mode in conducting media encounters an unsurmountable obstacle: the contamination with the particle-hole continuum (PHC) of excitations of the conductor; immediately Landau damps the TE mode [2]. In three dimensional (3D) electron liquids, within the Landau Fermi liquid, the Landau parameter $F_1^s > 6$ leads to an undamped TE mode outside the PHC [2]. But (i) such a large value of residual Coulomb interaction is not easy to realize in 3D electron systems and (ii) the conducting state is likely to undergo a phase transition into an ordered state, before such a strong interaction regime is reached [6].

Dirac materials are a new class of conductors where, instead of one band, two bands touch linearly [7–9]. Interband transitions in these systems contribute to the polarization response. In doped graphene, it has been predicted [10] and experimentally observed [11] that the unique void below the interband part of the PHC saves the TE mode of the vacuum from the Landau damping in a narrow frequency range and allows it to propagate through graphene [10,12–14]. The dispersion relation is quite close to the light dispersion [15] that makes Dirac matter potentially useful for the development of a broadband TE-pass polarizer [16–18]. Such TE modes are also expected in bilayer graphene [19] in a more pronounced way [19–21]. In undoped 3D Weyl semimetals, an additional vector \mathbf{b} exists that parametrizes the axion field [22] that gaps out one of the TE modes of the vacuum, but still it does not remedy the Landau damping [23]. Therefore, an *undamped* branch of TE mode in conducting media remains elusive. The

purpose of this paper is to show that the unique space-time structure that emerges in 2D TDMs (i) saves the TE mode from Landau damping by expelling it from the PHC. (ii) Unlike the case of doped graphene where the TE mode propagates at the speed of light, the present TE mode is sustained by charge density fluctuations propagating at fermionic velocity, v_F , and (iii) the TE mode in this new space-time structure of 2D TDMs can be sustained without doping.

Let us see how this happens. When the Dirac theory comes to mundane sub-eV energy scales of the band structure of solids, it can be modified in interesting ways, such as tilting the Dirac cone. The first realization of such tilting was in the α -(BEDT-TTF)₂I₃ organic salt under high pressure [24–26]. The $8pmmn$ borophene is also predicted to be stable TDM [27–30]. Quantum wells of LaAlO₃/LaNiO₃/LaAlO₃ also host tilted Dirac cone (TDC) and varying the number of LaNiO₃ monolayers can shift the Dirac node [31]. Smaller tilts can also be induced in graphene by mechanical deformation [32,33] and hydrogenation [34]. Tilted Dirac/Weyl fermions can also be realized in 3D systems transition metal dichalcogenide [35–38]. The tilt modifies many physical properties: apart from strong anisotropic conductivity [39], the tilt modifies the chiral anomaly [40] or can give rise to soft surface plasmon polaritons [41]. In 2D TDM, it induces a kink in the plasmons [42]. Additional linear plasmon modes in 2D [42,43] and type-II TDMs in 3D are predicted [44]. Other effects of tilt include anomalous magnetoplasmon and Hall effects [45,46], enhancement of superconductivity, and Josephson effect [47–49]. Many-body interactions in doped TDMs enhance the tilt perturbation [50,51].

One key observation is that TDMs *modify* the emergent Lorentz symmetry [35] of Dirac cones by producing a new space-time structure [52]. Covariance in this space-time is imprinted in the polarization tensor that determines the electromagnetic response of the system [53]. Therefore, at a very fundamental level, the structure of space-time in TDMs is different from traditional solid state systems [41,54–59]. In this work, we will show analytically that the tilt will remedy the

*jalali@physics.sharif.edu

†jafari@physics.sharif.edu

fundamental limitation of the conducting states by sustaining a genuine *undamped* TE collective mode that is sustained by charge fluctuations. We also establish that the rescue from damping has intimate connection with the new space-time structure in TDMS. For concreteness, we will focus on the 2D where the tilt and hence the space-time geometry is tunable by perpendicular electric fields [57].

This paper has been organized as follows. In Sec. II we review the standard theory of the propagation of electromagnetic modes on the surface of a 2D matter. Next, in Sec. III, we specifically focus on the 2DTDM with its unique space-time structure and derive their TE and TM mode dispersions. We investigate the possible propagation of TE mode in 2DTDMs and, finally, we discuss our result in Sec. V.

II. ELECTROMAGNETIC MODES AT INTERFACE

Consider a 2D matter at $z = 0$ surrounded by two media with dielectric constants ϵ_i , $i = 1, 2$. Imposing the standard boundary conditions on electric/magnetic field components at the interface of two media (see Appendixes A and B) gives the following traditional expressions for the dispersion relation of the TM and TE modes [10,12,60,61]:

$$\frac{\epsilon_1}{\gamma_1} + \frac{\epsilon_2}{\gamma_2} + \frac{4\pi i}{\omega q^2} \Gamma(\mathbf{q}, \omega) = 0 \quad (\text{TM mode}), \quad (1)$$

$$\gamma_1 + \gamma_2 - \frac{4\pi i \omega}{c^2 q^2} \Gamma'(\mathbf{q}, \omega) = 0 \quad (\text{TE mode}), \quad (2)$$

where c is the light velocity, ω is the frequency at which the wave is propagating, \mathbf{q} is the 2D wave vector in the xy plane (where the 2D matter lies), and the evanescent decay along the z direction surrounding media is encoded into $\gamma_i^2 = q^2 - \omega^2 \epsilon_i / c^2$. Note that the role of different dielectric constants ϵ_i is to give rise to harmonic and arithmetic averages of γ_i in the TM and TE modes, respectively. As we will see, for the solution generated by the new space-time structure, such variations in the dielectric properties do not change the qualitative picture. The functions $\Gamma(\mathbf{q}, \omega)$ and $\Gamma'(\mathbf{q}, \omega)$ relate to components $\sigma^{ab}(\mathbf{q}, \omega)$ of the conductivity tensor through

$$\Gamma(\mathbf{q}, \omega) = q_x^2 \sigma^{xx} + q_y^2 \sigma^{yy} + q_x q_y \sigma^{xy} + q_x q_y \sigma^{yx}, \quad (3)$$

$$\Gamma'(\mathbf{q}, \omega) = q_x^2 \sigma^{yy} + q_y^2 \sigma^{xx} - q_x q_y \sigma^{xy} - q_x q_y \sigma^{yx}. \quad (4)$$

Equation (1) results from imposing the boundary condition on \mathbf{H} field (see Appendix A) in the xy plane (and perpendicular to the propagation direction \mathbf{q} ; hence the name TM). In the nonretarded limit, $c \rightarrow \infty$, the TM mode reduces to the well-known result random phase approximation (RPA),

$$\epsilon^{\text{RPA}}(\mathbf{q}, \omega) = 1 - v(q)\chi(\mathbf{q}, \omega) = 0, \quad (5)$$

where $v(q) = 2\pi e^2 / q$ and $\chi(\mathbf{q}, \omega)$ is density-density correlation function and is related to the conductivity tensor σ^{ij} via the continuity equation [3]. The solution of the above TM-mode equation gives the collective excitations of charge density known as plasmon. These modes admit a straightforward intuition as collective charge motion [62,63].

The second dispersion given by Eq. (2) is the solution of electromagnetic field equations for the situation where the \mathbf{E} field lies perpendicular to \mathbf{q} in the plane of 2D matter. Such

modes, despite being very popular in waveguides [64], remain elusive in electron liquids, although in doped graphene, interband particle-hole excitations give a narrow frequency range $1.66 \lesssim \hbar\omega/\mu < 2$ set by the chemical potential (doping level) μ , which is typically a fraction of electron volt. But unfortunately their high speed $\sim c$ leads to poor confinement [10,12–14,19,60] of the graphene-based TE modes. One major advantage of our TE mode is that the new space-time structure of TDMS [41,52,53,57–59,65–67] provides a genuine opportunity for the propagation of TE mode that (i) is not limited by any doping scale and (ii) is strongly confined to 2D TDM due to its velocity scale v_F . Let us specialize Eq. (2) to TDMS to see how can this happen.

III. TE MODE EQUATION IN TDMS

The low energy excitations of tilted Dirac semimetals around one Dirac point in 2D are described by the following generic Hamiltonian:

$$H(k) = \hbar \begin{pmatrix} v_{x,t} k_x + v_{y,t} k_y & v_x k_x - i v_y k_y \\ v_x k_x + i v_y k_y & v_{x,t} k_x + v_{y,t} k_y \end{pmatrix}. \quad (6)$$

Here, $v_{x(y)}$ is the anisotropic Fermi velocity along $x(y)$ direction. Tilt of Dirac cone in each direction is defined by $v_{x,t}$ and $v_{y,t}$. The time reversal partner of the above Dirac cone (valley) has opposite tilt direction ($-v_{x(y),t}$). In the case of zero tilt $v_{x(y),t} = 0$, and assuming the isotropy condition $v_x = v_y = v_F$, the above Hamiltonian reduces to the effective theory of graphene. Parametrizing the tilt by $\boldsymbol{\zeta} = (\zeta_x, \zeta_y)$, where $v_{x(y),t} = \zeta_{x(y)} v_F$, one has

$$H(k) = \hbar v_F \begin{pmatrix} \zeta_x k_x + \zeta_y k_y & k_x - i k_y \\ k_x + i k_y & \zeta_x k_x + \zeta_y k_y \end{pmatrix}. \quad (7)$$

The energy eigenvalues $E_s = \hbar v_F k [1 + s\zeta \cos(\theta_t - \theta_k)]$ describe the conduction (valence) band for $s = + (-)$. The θ_k and θ_t are polar angles of the momentum and tilt vectors \mathbf{k} , $\boldsymbol{\zeta}$ with respect to the x axis and $k = |\mathbf{k}|$ and $\zeta = |\boldsymbol{\zeta}|$. As can be seen, in the presence of the tilt, $\boldsymbol{\zeta}$, the energy spectrum still remains linear in wave vector k , but the velocity depends on the direction. More fundamentally, the $\boldsymbol{\zeta}$ can be encoded into a suitable space-time metric [41,53–59].

What we need for the rest of the calculation is the conductivity tensor for TDC. It turns out that the new space-time structure allows one to express the polarization tensor in a covariant form [53] consistent with the Ward identity:

$$\Pi^{\mu\nu} = -[(q^2 - \Omega^2)g^{\mu\nu} - q^\mu q^\nu] \pi(q^2), \quad (8)$$

where the scalar part is $\pi(q) = -\frac{g_s v_F}{16\hbar \sqrt{q^2 - \Omega^2}}$ and the non-Minkowski metric is

$$g^{\mu\nu} = \begin{pmatrix} -1 & -\zeta_x & -\zeta_y \\ -\zeta_x & 1 - \zeta_x^2 & -\zeta_x \zeta_y \\ -\zeta_y & -\zeta_x \zeta_y & 1 - \zeta_y^2 \end{pmatrix}. \quad (9)$$

The (2+1)-dimensional energy-momentum vectors are $q_\mu = (-\omega/v_F, \mathbf{q})$, $q^\mu = g^{\mu\nu} q_\nu$, $q = |\mathbf{q}|$, $\Omega = \omega/v_F - \mathbf{q} \cdot \boldsymbol{\zeta}$ and g_s is

the spin degeneracy. Explicitly, the components are

$$\begin{aligned}\Pi^{00} &= \{q^2\}\pi(q), \quad \Pi^{0i} = \tilde{\Pi}^{0i} = \{q_i\Omega + q^2\zeta_i\}\pi(q), \\ \Pi^{ij} &= \{(\Omega^2 - q^2)\delta_{ij} + q_iq_j + q^2\zeta_i\zeta_j + \Omega q_i\zeta_j \\ &\quad + \Omega q_j\zeta_i\}\pi(q).\end{aligned}\quad (10)$$

The spatial components Π^{ij} of the above polarization are related to the conductivity tensor σ^{ij} required in Eqs. (3) and (4) by the standard relation $-i\omega\sigma^{ij} = e^2\Pi^{ij}$ [68,69]. Therefore, the Γ and Γ' functions needed in relations (1) and (2) are

$$-i\omega\Gamma(\mathbf{q}, \omega) = e^2\omega^2\Pi^{00}(\mathbf{q}, \Omega), \quad (11)$$

$$-i\omega\Gamma'(\mathbf{q}, \omega) = e^2q^2(\Omega^2 - q^2 + |\mathbf{q} \times \boldsymbol{\zeta}|^2)\pi(q). \quad (12)$$

As a consistency check, note that, in the long wavelength limit $q \rightarrow 0$, Eqs. (11) and (12) reduce to corresponding expressions derived by Mikhailov and Zeigler [10] for a single layer graphene. Let us put the above relations in a covariant form to reveal the peculiar role of the space-time (9):

$$\Pi_{\parallel}^{ab} = \hat{q}^a\hat{q}^b\omega^2\pi(q), \quad (13)$$

$$\Pi_{\perp}^{ab} = (\delta^{ab} - \hat{q}^a\hat{q}^b)[(\Omega^2 - q^2) + |\mathbf{q} \times \boldsymbol{\zeta}|^2]\pi(q), \quad (14)$$

where Latin indices stand for space indices. Comparison with (11) and (12) shows that indeed Γ and Γ' are proportional to longitudinal (Π_{\parallel}) and transverse (Π_{\perp}) parts of the polarization tensor. As can be seen the strength of the term due to tilt ζ is controlled by the charge fluctuation Π^{00} .

The dispersion of TM mode in Eq. (11) or (13) is governed by density fluctuations. The important difference with graphene is that ω is Doppler shifted to $\Omega = \omega/v_F - \boldsymbol{\zeta} \cdot \mathbf{q}$. In the $\zeta = 0$ case, it is well known that, when the average charge density is zero, this equation does not admit a solution in the singlet channel [70–73]. Likewise, the TM mode in the undoped TDC has no solution, unless a gate voltage [74–76] or chemical functionalization [77–79] dopes it. Then a plasmonic kink at the boundary of interband PHC and an additional overdamped linear plasmon branch appears [42,43].

The quantity Γ' governing the TE mode equation (12) or, equivalently, Eq. (14) is heavily affected by the tilt term which appears not only in Ω , but also as an explicit $\mathbf{q} \times \boldsymbol{\zeta}$ term (of strength Π^{00}) that stems from the covariant structure $\Pi^{\mu\nu}$ of Eq. (8) in the space-time (9). This empowers the TDMs to sustain a genuine undamped TE mode.

IV. PROPAGATION OF TE MODE IN TWO-DIMENSIONAL TDMs

First, let us clarify the role of doping in TDM. Mathematically, Eq. (2) may admit a propagating TE mode solution when the imaginary part of $\Gamma'(\mathbf{q}, \omega)$ is negative. Let us consider the doped case first. In 2D Dirac systems possessing upright Dirac cone (such as graphene), upon doping, a triangular shaped window below the interband and above the intraband PHC appears [71], which provides a chance for the formation of TE modes [10,12]. At $q \approx 0$ the formation of a solution for the TE mode is as follows: around the entire Fermi surface, at the excitation energy of 2μ , there will be plenty of particle-hole excitations that generate a negative and logarithmically singular imaginary part for the Γ' [10]. In the case of

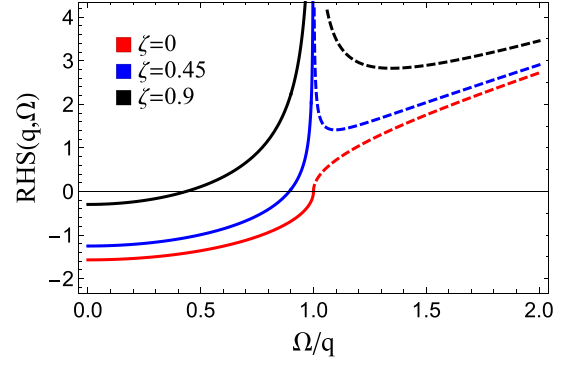


FIG. 1. Real (solid) and imaginary (dashed) parts of the right hand side in Eq. (17) for various values of tilt parameter, $\zeta = 0, 0.45, 0.9$ (red, blue, and black, respectively). Wave vector \mathbf{q} is perpendicular to $\boldsymbol{\zeta}$. The imaginary part is nonzero for $\Omega > q$ corresponding to PHC.

TDC, at $q \approx 0$, depending on the angle at which the initial \mathbf{k} state from valence band is picked, the excitation energy will deviate from 2μ . This smearing around 2μ will destroy the logarithmic singularity as shown in Fig. 2 of Appendix C. As long as dielectric constants in both sides are the same, one still gets a solution corresponding to $\gamma = 0$, which is nothing but the TE mode of the surrounding dielectric medium that has escaped the damping due to a void in the PHC. In this way, the TE mode of graphene will survive, but will evolve in TDM in two respects: (i) its velocity will be closer to c and (ii) its frequency range will be even more limited.

Therefore, let us next consider an undoped 2D TDC system. In this case, from Eq. (12) the TE mode equation becomes

$$\gamma_1 + \gamma_2 + \frac{4\pi e^2}{c^2}(\Omega^2 - q^2 + |\mathbf{q} \times \boldsymbol{\zeta}|^2)\pi(q)\Theta(q - \Omega) = 0. \quad (15)$$

Here, we added a step function to the definition of Γ' to pick a region in which the imaginary part of Π^{ij} in Eq. (10) (and hence the real part of Γ') is zero. To understand the structure of Eq. (15), first we consider its $\zeta \rightarrow 0$ limit:

$$\gamma_1 + \gamma_2 + \frac{4\pi e^2}{c^2 v_F^2}(\omega^2 - v_F^2 q^2)\pi(q)\Theta(v_F q - \omega) = 0. \quad (16)$$

The second term in the above equation is nonzero only when $v_F q > \omega$. In this regime $\omega^2 - v_F^2 q^2$ is negative. But since $\pi(q)$ itself is also negative, the above equation admits no solution. Therefore, in upright Dirac cone systems, the only way to get an undamped TE mode is to inject free charge carriers into it [10,12,80]. In TDMs, the $\mathbf{q} \times \boldsymbol{\zeta}$ term arising from the structure of the space-time generates an undamped TE mode even at zero doping. Substituting for $\pi(q)$ in Eq. (15) gives

$$\frac{c\gamma}{\alpha} = \frac{\pi}{4} \frac{\Theta(q - \Omega)}{\sqrt{q^2 - \Omega^2}} (\Omega^2 - q^2 + |\mathbf{q} \times \boldsymbol{\zeta}|^2). \quad (17)$$

The $\alpha = e^2/\hbar c = 1/137$ is the fine structure constant and $\gamma = (\gamma_1 + \gamma_2)/2$ is the average of the confinement length of the mode in two sides of the 2D material. Figure 1 shows how tilt generates a solution for Eq. (17). Solid lines are the real part

of the right-hand side (RHS) for indicated values of ζ . As can be seen, the presence of tilt generates an inverse square divergence (reminiscent of bound state formation in 1D problems) that will be able to intersect the LHS and gives a solution for $\Omega/q < 1$. The solution suggested by Fig. 1 for $\Omega < q$ can be analytically obtained up to leading order in v_F/c ,

$$\Omega = \omega - v_F \mathbf{q} \cdot \boldsymbol{\zeta} = v_F q - \frac{v_F q}{32} \left(\frac{\pi \alpha v_F}{c} \right)^2 |\hat{\mathbf{q}} \times \boldsymbol{\zeta}|^4, \quad (18)$$

where the first term in the RHS corresponds to the lower edge of the PHC. There are two important points to be noted here. (i) The principal velocity scale of this TE mode is set by v_F and not by c . This readily implies $\gamma \sim q$ and therefore the confinement length is set by the wavelength. This can be useful in optoelectronic applications [72,81]. (ii) Clearly the $\mathbf{q} \times \boldsymbol{\zeta}$ term arising from the structure of the space-time has brought the energy of this TE mode below the PHC. This is how tilt can generate a genuine and confinable TE mode sustained by collective charge fluctuations in the material. Notice that, when the propagation direction is along the tilt direction, $\boldsymbol{\zeta}$, the TE mode will be tangent to the lower border of the PHC and acquires damping. This effect can be utilized to optically identify the tilt direction, as the direction $\boldsymbol{\zeta}$ will be the only direction along which our TE mode ceases to propagate.

V. SUMMARY AND DISCUSSION

In this paper, starting from a covariant expression for the polarization of an *undoped* two-dimensional TDM in a space-time given by metric (9), we have investigated the formation of a genuine TE collective mode. The TE mode equation is augmented by $\mathbf{q} \times \boldsymbol{\zeta}$ term which arises from the structure of the space-time whose coefficient is the charge fluctuation Π^{00} . As such, Π^{00} manifests not only as plasmons, but also as TE modes in TDMs. The most manifest form of this effect can take place for $\mathbf{q} \perp \boldsymbol{\zeta}$. Due to this new term, the TE mode manages to escape from the contamination with the PHC of the TDM. The velocity of the resulting mode is determined by v_F . Therefore, in contrast to the case of graphene [10], the present TE mode will be sharply confined to the 2D TDM which can be used to *sharply focus* the TE mode into a 2D plane. A further advantage of our TE mode is that, while in doped graphene the TE mode is very fragile and goes away by turning on a difference in the dielectric constants of the surrounding media [82], our TE mode being sustained by matter density fluctuations is not sensitive to possible difference in the dielectric constants of the surrounding media. This proves to be very convenient for settings where TDM is mounted on a substrate. Furthermore, the huge velocity difference for the TE mode in TDM and the vacuum leads to a transmission coefficient of $\tau = 4v_F/c$ [83], which distinguishes the propagation of TE mode in TDM from the one in the substrate as a huge refractive index medium. An important feature of our TE mode is that it is sustained by the *fluctuations* of the charge density, in a system at the charge neutrality point where the *average* density of the (free) charge carriers is zero. Shallow bound state character of this TE mode with respect to the lower edge of the PHC implies that its spatial extent is much larger than the lattice scales. Hence the potential disorder can not efficiently scatter it. The temperature leads

to an effective doping via the temperature dependence of the chemical potential which damps the TE mode for $\hbar\omega \lesssim k_B T$. But since there is no other scale except for the high energy cutoff defining the Dirac theory, the TE mode continues to propagate at energy scales above the $k_B T$.

Finally, let us comment about the other valley which is inevitably present in TDM and corresponds to $-\boldsymbol{\zeta}$. Since the transverse polarization involves the square of $\mathbf{q} \times \boldsymbol{\zeta}$, the presence of the other valley does not destroy the TE mode. Indeed, adding the contribution of the other valley with $-\boldsymbol{\zeta}$ doubles the degrees of freedom and so one might expect two TE modes. But due to opposite Doppler shift, the additional peak from the other valley (cf., Fig. 1) will be *inside* the PHC, and hence gets damped. Therefore, even in the presence of the other valley, one undamped TE mode branch continues to exist. The question of possible intervalley modes remains open and pertinent.

ACKNOWLEDGMENTS

S.A.J. appreciates research deputy of Sharif University of Technology, Grant No. G960214.

APPENDIX A: TRANSVERSE MAGNETIC MODE

In this section, we give more detail on the derivation of the transverse magnetic mode dispersion relation in TDMs. Suppose the 2D TDM located in xy plane at $z = 0$ and surrounded by two media with dielectric constant ϵ_1, ϵ_2 and the propagation of electric and magnetic field along the z axis in surrounding media has evanescent behavior described with γ . As it has been mentioned in the body of the paper, the electromagnetic TM mode propagates at the interface with the magnetic field also lying in the xy plane and perpendicular to the wave vector. This implies $H_{i,z} = 0$ in which $i = 1, 2$ stands for upper $z > 0$ and lower half-plane $z < 0$:

$$\begin{aligned} \mathbf{H}_i &= (H_{i,x}, H_{i,y}, 0) e^{i(\mathbf{q}\mathbf{r} - \omega t)} e^{-\gamma_i |z|}, \\ \mathbf{E}_i &= (E_{i,x}, E_{i,y}, E_{i,z}) e^{i(\mathbf{q}\mathbf{r} - \omega t)} e^{-\gamma_i |z|}, \\ \mathbf{q} &= (q_x, q_y). \end{aligned} \quad (A1)$$

In the bulk of two media as a result of no free charge and current the Maxwell equation finds the following representation:

$$\begin{aligned} \nabla \cdot \mathbf{D} &= \rho \delta(z), \quad \nabla \cdot \mathbf{B} = 0, \\ \nabla \times \mathbf{E} &= -\frac{1}{c} \partial_t \mathbf{B}, \quad \nabla \times \mathbf{B} = \frac{1}{c} \partial_t \mathbf{D}. \end{aligned} \quad (A2)$$

For ease of calculation we suppose two media are the same without any magnetic properties; hence we have $\epsilon_1 = \epsilon_2 = \epsilon_0$ and $\mu_1 = \mu_2 = \mu_0$. These properties imply that $\mathbf{D}_i = \epsilon_0 \mathbf{E}_i$ and $\mathbf{H}_i = \mathbf{B}_i / \mu_0$. Hence the homogeneous equation for the electric and magnetic field in the bulk is given by

$$\nabla \times \nabla \times \mathbf{E} = -\frac{1}{c^2} \partial_t^2 \mathbf{E}. \quad (A3)$$

Inserting the definition of electric field components in the above relation gives

$$\begin{bmatrix} q_y^2 - \gamma_i^2 & -q_x q_y & \mp i q_x \gamma_i \\ -q_x q_y & q_x^2 - \gamma_i^2 & \mp i q_y \gamma_i \\ \mp i q_x \gamma_i & \mp i q_y \gamma_i & q_x^2 + q_y^2 \end{bmatrix} \mathbf{E} - \frac{\omega^2}{c^2} \epsilon_i \mathbf{E} = 0. \quad (A4)$$

The determinant of the above matrix for two media with the same dielectric constant defines the same decay constant $\gamma_1^2 = \gamma_2^2 = q^2 - \omega^2/c^2$. The dispersion of electromagnetic modes can be derived from boundary conditions at $z = 0$, where the tilted Dirac plane is located:

$$\begin{aligned} E_{1,t} = E_{2,t} &\Rightarrow E_{1,x} = E_{2,x}, \quad E_{1,y} = E_{2,y}, \\ D_{1,n} - D_{2,n} &= 4\pi\rho\delta(z) \Rightarrow E_{1,z} - E_{2,z} = 4\pi\rho\delta(z), \\ H_{1,n} = H_{2,n} &\Rightarrow H_{1,z} = H_{2,z}, \\ H_{1,t} - H_{2,t} &= \frac{4\pi}{c} \mathbf{J} \times \hat{n} \\ \Rightarrow H_{1,x} - H_{2,x} &= \frac{4\pi}{c} J_y, \quad H_{1,y} - H_{2,y} = -\frac{4\pi}{c} J_x. \end{aligned} \quad (\text{A5})$$

The current vector is related to the electric field vector by conductivity tensor as

$$\mathbf{J} = \begin{bmatrix} \sigma^{xx}(\mathbf{q}, \omega) & \sigma^{xy}(\mathbf{q}, \omega) \\ \sigma^{yx}(\mathbf{q}, \omega) & \sigma^{yy}(\mathbf{q}, \omega) \end{bmatrix} \begin{bmatrix} E_x \\ E_y \end{bmatrix}. \quad (\text{A6})$$

Moreover, in each medium, the field equations are

$$\nabla \cdot \mathbf{H} = 0 \Rightarrow iq_x H_{i,x} + iq_y H_{i,y} \mp \gamma_i H_{i,z} = 0, \quad (\text{A7})$$

$$\begin{aligned} \nabla \times \mathbf{E} &= -\frac{1}{c} \partial_t \mathbf{B} \Rightarrow i\omega H_{i,x} = \pm \gamma_i E_{i,y}, \\ i\omega H_{i,y} &= \mp \gamma_i E_{i,x}, \quad \omega H_{i,z} = q_x E_{i,y} + q_y E_{i,x}, \end{aligned} \quad (\text{A8})$$

in which the minus (plus) sign stands for $i = 1(2)$.

Using the boundary condition equation for a normal component of electric field (E_z), Eq. (A5), and implementing with the continuity equation one finds

$$E_{1,z} - E_{2,z} = \frac{4\pi}{i\omega c^2} (q_x j_x + q_y j_y). \quad (\text{A9})$$

Gauss's law for electric field in each medium ($i = 1, 2$) can be rewritten as

$$iq_x E_{i,x} + iq_y E_{i,y} \mp \gamma_i E_{i,z} = 0. \quad (\text{A10})$$

Combination of Eqs. (A9) and (A10) gives rise to the following relation:

$$\begin{aligned} E_{1,x} \left[q_x + \frac{2\pi i\gamma}{c^2\omega} (q_x \sigma^{xx} + q_y \sigma^{yx}) \right] \\ + E_{1,y} \left[q_y + \frac{2\pi i\gamma}{c^2\omega} (q_x \sigma^{xy} + q_y \sigma^{yy}) \right] = 0. \end{aligned} \quad (\text{A11})$$

Using $\nabla \cdot \mathbf{B} = 0$ and Faraday's law we find

$$q_x E_{i,y} = q_y E_{i,x}. \quad (\text{A12})$$

Combination of (A11) and (A12) gives the TM dispersion relation as

$$1 + \frac{2\pi i\gamma}{\omega q^2} \Gamma(\mathbf{q}, \omega) = 0, \quad (\text{A13})$$

where

$$\Gamma(\mathbf{q}, \omega) = q_x^2 \sigma^{xx}(\mathbf{q}, \omega) + q_y^2 \sigma^{yy}(\mathbf{q}, \omega) + 2q_x q_y \sigma^{xy}(\mathbf{q}, \omega). \quad (\text{A14})$$

Inserting each element of conductivity tensor using $-i\omega\sigma^{ij} = e^2 \Pi^{ij}$ and (10) we find the following dispersion for TM mode:

$$1 - \frac{2\pi e^2 \gamma}{q^2} \Pi^{00}(\mathbf{q}, \Omega) = 0. \quad (\text{A15})$$

Not surprisingly, in the instantaneous limit $c \rightarrow \infty$ above TM dispersion relation reduces to that of plasmon in RPA:

$$1 - v(q)\Pi^{00}(\mathbf{q}, \Omega) = 0. \quad (\text{A16})$$

Indeed when the magnetic field is in the xy (2D matter) plane the longitudinal component of electric field E_{\parallel} , which is parallel with the propagation direction of electromagnetic field within dipole electric wave, induces longitudinal charge oscillation, well known as the plasmon mode.

APPENDIX B: TRANSVERSE ELECTRIC MODE

In the case of transverse electric field derivation, we supposed the electric field is in the xy surface and is perpendicular to the propagation direction of electromagnetic wave, which implies $E_{i,z} = 0$ in both media. Hence, generally, the electric and magnetic fields have the following representation as

$$\begin{aligned} \mathbf{E}_i &= (E_{i,x}, E_{i,y}, 0) e^{i(\mathbf{q}\cdot\mathbf{r} - \omega t)} e^{-\gamma_i |z|}, \\ \mathbf{H}_i &= (H_{i,x}, H_{i,y}, H_{i,z}) e^{i(\mathbf{q}\cdot\mathbf{r} - \omega t)} e^{-\gamma_i |z|}, \\ \mathbf{q} &= (q_x, q_y), \end{aligned} \quad (\text{B1})$$

where $i = 1, 2$ stands for upper $z > 0$ and lower half space $z < 0$, as before, and γ encodes the evanescent behavior of propagating electromagnetic modes along the z direction.

The boundary condition for magnetic field in Eq. (A5) and Faraday's law for the normal component of magnetic field in each medium gives rise to the following relation:

$$q_x H_{1,x} + q_y H_{1,y} = \frac{2\pi}{c} (q_x J_y - q_y J_x). \quad (\text{B2})$$

Inserting the definition of $H_{1,x}$ and $H_{1,y}$ from Faraday's law, the dispersion relation of TE mode can be derived as

$$1 - \frac{2\pi i\omega}{c^2 \gamma q^2} \Gamma'(\mathbf{q}, \omega), \quad (\text{B3})$$

in which

$$\Gamma'(\mathbf{q}, \omega) = q_x^2 \sigma^{yy}(\mathbf{q}, \omega) + q_y^2 \sigma^{xx}(\mathbf{q}, \omega) - 2q_x q_y \sigma^{xy}(\mathbf{q}, \omega). \quad (\text{B4})$$

It is also possible to represent the above dispersion relation versus components of the polarization tensor by using Eq. (10) of the main text.

APPENDIX C: DOPED TILTED DIRAC

Here in this section we give more detail on the calculation of optical conductivity in doped tilted Dirac materials. A peculiar type of low energy excitations in doped Dirac materials provides two different channels for particle hole excitations and consequently optical responses consist of intra- and interband parts, which are given by the following relations:

$$\begin{aligned}\sigma_{\text{intra}}^{\alpha\beta}(\omega) &= \frac{-ie^2}{\hbar^2\omega^+A} \sum_{k,\lambda=\pm} \frac{\partial E_\lambda(k)}{\partial k_\alpha} \frac{\partial f(E_\lambda(k))}{\partial E_\lambda(k)} \frac{\partial E_\lambda(k)}{\partial k_\beta}, \\ \sigma_{\text{inter}}^{\alpha\beta}(\omega) &= \frac{ie^2\hbar}{A} \sum_{k,\lambda=\pm} \frac{f(E_\lambda(k)) - f(E_{-\lambda}(k))}{E_\lambda(k) - E_{-\lambda}(k) - \hbar(\omega + i0^+)} \frac{\langle k, \lambda | v_\alpha | k, -\lambda \rangle \langle k, -\lambda | v_\beta | k, \lambda \rangle}{E_\lambda(k) - E_{-\lambda}(k)}.\end{aligned}\quad (\text{C1})$$

Here, $\omega^+ = \omega + i0^+$ and A is the area of the sample. Searching for the propagation of the TE mode, we suppose the wave vector $\mathbf{q} = q\hat{x}$ in Eq. (B4), which gives

$$\Gamma'(\omega) = q^2\sigma^{yy}(\omega).\quad (\text{C2})$$

This represents that the only required component of optical conductivity is σ^{yy} ; therefore, in the following we focus on its intra- and intercomponent of σ^{yy} and suppose tilt direction, with respect to the x axis, is given by θ_t . The intraband component is given by

$$\begin{aligned}\sigma_{\text{intra}}^{yy}(\omega) &= \frac{ie^2v_F^2}{\omega^+} \sum_{k,\lambda=\pm} \left(\zeta_y + \lambda \frac{k_y}{k} \right)^2 \delta(\mu - \hbar v_F(\boldsymbol{\zeta} \cdot \mathbf{k} + \lambda k)) \\ &= \frac{ie^2v_F}{\omega^+} \sum_k (\zeta_y + \sin\theta)^2 \frac{\delta(k - k_0)}{1 + \zeta \cos(\theta - \theta_t)} \\ &= \frac{ie^2\mu}{\hbar^2 4\pi^2 \omega^+} \int_0^{2\pi} d\theta \frac{(\zeta_y + \sin\theta)^2}{[1 + \zeta \cos(\theta - \theta_t)]^2},\end{aligned}\quad (\text{C3})$$

where $k_0 = \mu/\hbar v_F[1 + \zeta \cos(\theta - \theta_t)]$. The above expression simplifies to

$$\sigma_{\text{intra}}^{yy}(\omega) = \frac{ie^2\mu}{\hbar^2 4\pi \omega^+} \left\{ -\frac{2}{\zeta^2} \cos 2\theta_t + \frac{1}{(1 - \zeta^2)^{3/2}} [1 - 2\zeta^2 \sin^2 \theta_t + \cos 2\theta_t (2/\zeta^2 - 3)] \right\}.\quad (\text{C4})$$

The interband term is given by

$$\begin{aligned}\sigma_{\text{inter}}^{yy}(\omega) &= \frac{ie^2}{2A} \sum_k \frac{1 + \cos 2\theta}{2\hbar v_F k} \left[\frac{f(E_+(k)) - 1}{2v_F k - \omega^+} - \frac{f(E_+(k)) - 1}{2v_F k + \omega^+} \right] \\ &= \frac{e^2}{16\pi\hbar} \left\{ \Theta(1 - X_-^2) \left(\theta_- - \frac{1}{2} \cos 2\theta_t \sin 2\theta_- \right) + \pi \Theta(-X_- - 1) + i \cos^2 \theta_t C(\omega) - i \cos 2\theta_t D(\omega) \right\},\end{aligned}\quad (\text{C5})$$

in which $\theta_- = \arccos X_-$ and $X_- = (2\mu - \hbar\omega)/\hbar\omega\zeta$,

$$\begin{aligned}D(\omega) &= [g(x) - f(x) - l(x)]|_0^1 - [l(x) - g(x) + f(x)]|_{-1}^0 \Theta[\omega(1 - \zeta) - 2\mu] \\ &\quad + [g(0) - l(0) - f(0) + 1] \Theta[2\mu - \omega(1 - \zeta)] [f(-1) + g(-1) - l(-1) - 1] \Theta[2\mu - \omega(1 + \zeta)],\end{aligned}\quad (\text{C6})$$

and

$$C(\omega) = -2l(-1)\Theta[2\mu - \omega(1 + \zeta)] - 2l(0)\Theta[2\mu - \omega(1 - \zeta)] + 2[l(-1) - l(0)]\Theta[\omega(1 - \zeta) - 2\mu] - 2[l(-1) - l(0)],$$

with

$$\begin{aligned}l(x) &= \ln \left[\frac{\omega + 2\mu x}{\zeta\omega} + \sqrt{\left(\frac{\omega + 2\mu x}{\zeta\omega} \right)^2 - 1} \right], \\ f(x) &= \left(\frac{\omega + 2\mu x}{\zeta\omega} \right)^2, \\ g(x) &= \left(\frac{\omega + 2\mu x}{\zeta\omega} \right) \sqrt{\left(\frac{\omega + 2\mu x}{\zeta\omega} \right)^2 - 1}.\end{aligned}$$

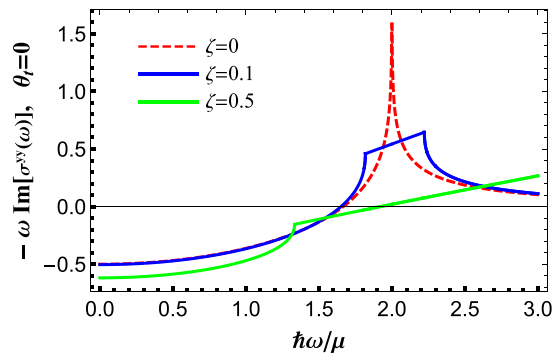


FIG. 2. Imaginary part of $\omega\sigma^{yy}(\omega)$ for different values of tilt parameter. Note that we supposed tilt vector along the x axis, i.e., $\theta_t = 0$. Here, the red dashed line corresponds to the upright Dirac cone $\zeta = 0$; blue and green solid lines stand for $\zeta = 0.1, 0.5$, respectively.

Based on the TE dispersion relation in Eq. (2), if $i\omega\Gamma'$ or $-\omega\text{Im}\Gamma'$ becomes positive, a solution can be possible. This quantity has been plotted in Fig. 2 for various values of the tilt parameter ζ . As can be seen the effect of tilt is to kill the logarithmic singularity (dashed line) and push the positive support of the function to higher frequencies. Therefore, analogous to doped graphene, the TE mode in doped TDM can also propagate, but in a more limited window of frequencies. Again the propagation velocity in the present doped case will be closer to the velocity c of the light as the positive portion of the above curve is to be compared with $\sim c\gamma$, which is consistent with the $\gamma \approx 0$ solution. This is again nothing but the TE mode of the surrounding media. The dependence of the above curves on the angle θ is weak and does not produce significant difference.

- [1] J. D. Jackson, *Classical Electrodynamics* (Wiley, New York, 1999).
- [2] D. Pines and P. Nozières, *Theory of Quantum Liquids: Normal Fermi Liquids* (Avalon Publishing, New York, 1966).
- [3] G. Giuliani and G. Vignale, *Quantum Theory of The Electron Liquid* (Cambridge University Press, Cambridge, UK, 2005).
- [4] A. Hill, S. A. Mikhailov, and K. Ziegler, *EPL (Europhys. Lett.)* **87**, 27005 (2009).
- [5] V. Kadirko, K. Ziegler, and E. Kogan, *Graphene* **02**, 97 (2013).
- [6] S. Sachdev, *Quantum Phase Transitions* (Cambridge University Press, Cambridge, UK, 2011).
- [7] T. O. Wehling, A. M. Black-Schaffer, and A. V. Balatsky, *Adv. Phys.* **63**, 1 (2014).
- [8] N. P. Armitage, E. J. Mele, and A. Vishwanath, *Rev. Mod. Phys.* **90**, 015001 (2018).
- [9] A. H. Castro Neto, F. Guinea, N. M. R. Peres, K. S. Novoselov, and A. K. Geim, *Rev. Mod. Phys.* **81**, 109 (2009).
- [10] S. A. Mikhailov and K. Ziegler, *Phys. Rev. Lett.* **99**, 016803 (2007).
- [11] S. G. Menabde, D. R. Mason, E. E. Kornev, C. Lee, and N. Park, *Sci. Rep.* **6**, 21523 (2016).
- [12] Z. Jalali-Mola and S. Jafari, *J. Magn. Magn. Mater.* **471**, 220 (2019).
- [13] O. Kotov, M. Kol'chenko, and Y. E. Lozovik, *Opt. Express* **21**, 13533 (2013).
- [14] Y. Bludov, A. Ferreira, N. M. R. Peres, and M. I. Vasilevskiy, *Int. J. Mod. Phys. B* **27**, 1341001 (2013).
- [15] Small deviation from the light speed is due to the presence of a one atom thick graphene.
- [16] M. Jablan, H. Buljan, and M. Soljačić, *Phys. Rev. B* **80**, 245435 (2009).
- [17] F. M. D. Pellegrino, G. G. N. Angilella, and R. Pucci, *Phys. Rev. B* **84**, 195407 (2011).
- [18] Q. Bao, H. Zhang, B. Wang, Z. Ni, C. H. Y. X. Lim, Y. Wang, D. Y. Tang, and K. P. Loh, *Nat. Photon.* **5**, 411 (2011).
- [19] M. Jablan, H. Buljan, and M. Soljačić, *Opt. Express* **19**, 11236 (2011).
- [20] G. Gómez-Santos and T. Stauber, *EPL (Europhys. Lett.)* **99**, 27006 (2012).
- [21] T. Stauber and G. Gómez-Santos, *Phys. Rev. B* **85**, 075410 (2012).
- [22] X.-L. Qi and S.-C. Zhang, *Phys. Today* **63**, 33 (2010).
- [23] Y. Ferreira and A. Cortijo, *Phys. Rev. B* **93**, 195154 (2016).
- [24] K. Kajita, T. Ojio, H. Fujii, Y. Nishio, H. Kobayashi, A. Kobayashi, and R. Kato, *J. Phys. Soc. Jpn.* **61**, 23 (1992).
- [25] S. Katayama, A. Kobayashi, and Y. Suzumura, *J. Phys. Soc. Jpn.* **75**, 054705 (2006).
- [26] K. Kajita, Y. Nishio, N. Tajima, Y. Suzumura, and A. Kobayashi, *J. Phys. Soc. Jpn.* **83**, 072002 (2014).
- [27] X.-F. Zhou, X. Dong, A. R. Oganov, Q. Zhu, Y. Tian, and H.-T. Wang, *Phys. Rev. Lett.* **112**, 085502 (2014).
- [28] A. D. Zabolotskiy and Y. E. Lozovik, *Phys. Rev. B* **94**, 165403 (2016).
- [29] A. Lopez-Bezanilla and P. B. Littlewood, *Phys. Rev. B* **93**, 241405(R) (2016).
- [30] B. Feng, O. Sugino, R.-Y. Liu, J. Zhang, R. Yukawa, M. Kawamura, T. Iimori, H. Kim, Y. Hasegawa, H. Li, L. Chen, K. Wu, H. Kumigashira, F. Komori, T.-C. Chiang, S. Meng, and I. Matsuda, *Phys. Rev. Lett.* **118**, 096401 (2017).
- [31] L. L. Tao and E. Y. Tsybal, *Phys. Rev. B* **98**, 121102(R) (2018).
- [32] M. O. Goerbig, J.-N. Fuchs, G. Montambaux, and F. Piéchon, *Phys. Rev. B* **78**, 045415 (2008).
- [33] J. L. Mañes, F. de Juan, M. Sturla, and M. A. H. Vozmediano, *Phys. Rev. B* **88**, 155405 (2013).
- [34] H.-Y. Lu, A. S. Cuamba, S.-Y. Lin, L. Hao, R. Wang, H. Li, Y. Y. Zhao, and C. S. Ting, *Phys. Rev. B* **94**, 195423 (2016).
- [35] M. Yan, H. Huang, K. Zhang, E. Wang, W. Yao, K. Deng, G. Wan, H. Zhang, M. Arita, H. Yang, Z. Sun, H. Yao, Y. Wu, S. Fan, W. Duan, and S. Zhou, *Nat. Commun.* **8**, 257 (2017).
- [36] H.-J. Noh, J. Jeong, E.-J. Cho, K. Kim, B. I. Min, and B.-G. Park, *Phys. Rev. Lett.* **119**, 016401 (2017).
- [37] A. A. Soluyanov, D. Gresch, Z. Wang, Q. Wu, M. Troyer, X. Dai, and B. A. Bernevig, *Nature (London)* **527**, 495 (2015).
- [38] Z. Wang, D. Gresch, A. A. Soluyanov, W. Xie, S. Kushwaha, X. Dai, M. Troyer, R. J. Cava, and B. A. Bernevig, *Phys. Rev. Lett.* **117**, 056805 (2016).
- [39] S. Rostamzadeh, I. Adagideli, and M. O. Goerbig, *Phys. Rev. B* **100**, 075438 (2019).

- [40] K. Zhang, E. Zhang, M. Xia, P. Gao, and S. Zhang, *Ann. Phys. (NY)* **394**, 1 (2018).
- [41] Z. Jalali-Mola and S. A. Jafari, *Phys. Rev. B* **100**, 205413 (2019).
- [42] Z. Jalali-Mola and S. A. Jafari, *Phys. Rev. B* **98**, 195415 (2018).
- [43] Z. Jalali-Mola and S. A. Jafari, *Phys. Rev. B* **98**, 235430 (2018).
- [44] K. Sadhukhan, A. Politano, and A. Agarwal, *Phys. Rev. Lett.* **124**, 046803 (2020).
- [45] J. Sári, C. Tóke, and M. O. Goerbig, *Phys. Rev. B* **90**, 155446 (2014).
- [46] A. A. Zyuzin and R. P. Tiwari, *JETP Lett.* **103**, 717 (2016).
- [47] Z. Faraei and S. A. Jafari, *Phys. Rev. B* **100**, 245436 (2019).
- [48] Z. Faraei and S. Jafari, *Phys. Rev. B* **101**, 214508 (2020).
- [49] M. Alidoust, K. Halterman, and A. A. Zyuzin, *Phys. Rev. B* **95**, 155124 (2017).
- [50] P.-L. Zhao and A.-M. Wang, *Phys. Rev. B* **100**, 125138 (2019).
- [51] Y.-W. Lee and Y.-L. Lee, *Phys. Rev. B* **97**, 035141 (2018).
- [52] S. A. Jafari, *Phys. Rev. B* **100**, 045144 (2019).
- [53] Z. Jalali-Mola and S. A. Jafari, *Phys. Rev. B* **100**, 075113 (2019).
- [54] G. E. Volovik, *JETP Lett.* **104**, 645 (2016).
- [55] K. Zhang and G. E. Volovik, *JETP Lett.* **105**, 519 (2017).
- [56] G. E. Volovik, *Phys. Usp.* **61**, 89 (2018).
- [57] T. Farajollahpour, Z. Faraei, and S. A. Jafari, *Phys. Rev. B* **99**, 235150 (2019).
- [58] K. Hashimoto and Y. Matsuo, *Phys. Rev. B* **102**, 195128 (2020).
- [59] Y. Kedem, E. J. Bergholtz, and F. Wilczek, [arXiv:2001.02625](https://arxiv.org/abs/2001.02625) [cond-mat.mes-hall].
- [60] M. Nakayama, *J. Phys. Soc. Jpn.* **36**, 393 (1974).
- [61] S. A. Maier, *Plasmonics: Fundamentals and Applications* (Springer Science & Business Media, New York, 2007).
- [62] A. L. Fetter, *Ann. Phys. (NY)* **81**, 367 (1973).
- [63] A. Lucas and S. Das Sarma, *Phys. Rev. B* **97**, 115449 (2018).
- [64] K. Okamoto, *Fundamentals of Optical Waveguides*, 2nd ed. (Academic Press, New York, 2006).
- [65] H. Huang, K.-H. Jin, and F. Liu, *Phys. Rev. B* **98**, 121110(R) (2018).
- [66] M. Kang, H. Huang, S. Zhang, H. Xu, and F. Liu, [arXiv:1908.05049](https://arxiv.org/abs/1908.05049).
- [67] H. Liu, J.-T. Sun, H. Huang, F. Liu, and S. Meng, [arXiv:1809.00479](https://arxiv.org/abs/1809.00479).
- [68] X. G. Wen, *Quantum Field Theory of Many-Body Systems* (Oxford University Press, Oxford, 2004).
- [69] J. Sólyom, *Fundamentals of the Physics of Solids: Volume 3—Normal, Broken-Symmetry, and Correlated Systems* (Springer Science & Business Media, New York, 2010).
- [70] B. Wunsch, T. Stauber, F. Sols, and F. Guinea, *New J. Phys.* **8**, 318 (2006).
- [71] E. H. Hwang and S. Das Sarma, *Phys. Rev. B* **75**, 205418 (2007).
- [72] A. Grigorenko, M. Polini, and K. Novoselov, *Nat. Photon.* **6**, 749 (2012).
- [73] Although a solution can be generated by including the Stoner fluctuations corresponding to ladder diagrams [12,84], or by including thermal fluctuations to generate thermoplasmons [85,86].
- [74] K. S. Novoselov, A. K. Geim, S. V. Morozov, D. Jiang, Y. Zhang, S. V. Dubonos, I. V. Grigorieva, and A. A. Firsov, *Science* **306**, 666 (2004).
- [75] F. Wang, Y. Zhang, C. Tian, C. Girit, A. Zettl, M. Crommie, and Y. R. Shen, *Science* **320**, 206 (2008).
- [76] J. Chen, M. Badioli, P. Alonso-González, S. Thongrattanasiri, F. Huth, J. Osmond, M. Spasenović, A. Centeno, A. Pesquera, P. Godignon *et al.*, *Nature (London)* **487**, 77 (2012).
- [77] D. W. Boukhvalov and M. I. Katsnelson, *Nano Lett.* **8**, 4373 (2008).
- [78] D. W. Boukhvalov and M. I. Katsnelson, *J. Phys.: Condens. Matter* **21**, 344205 (2009).
- [79] T. Kuila, S. Bose, A. K. Mishra, P. Khanra, N. H. Kim, and J. H. Lee, *Prog. Mater. Sci.* **57**, 1061 (2012).
- [80] Note that, although the part of transverse polarization (14) that does not involve $\mathbf{q} \times \boldsymbol{\zeta}$ does indeed produce a transverse electric field polarization, this mode does not survive the contamination with the (interband) PHC of the material. If there was no material, there would be no contamination, and therefore this part of Π_{\perp} would be enough to let the TE mode propagate in vacuum.
- [81] A. Vakil and N. Engheta, *Science* **332**, 1291 (2011).
- [82] A. Gutiérrez-Rubio, T. Stauber, and F. Guinea, *J. Opt.* **15**, 114005 (2013).
- [83] H. Georgi, *The Physics of Waves* (Prentice-Hall, Englewood Cliffs, NJ, 1993).
- [84] S. Gangadharaiah, A. M. Farid, and E. G. Mishchenko, *Phys. Rev. Lett.* **100**, 166802 (2008).
- [85] O. Vafek, *Phys. Rev. Lett.* **97**, 266406 (2006).
- [86] S. Das Sarma and Q. Li, *Phys. Rev. B* **87**, 235418 (2013).